Stability Analysis of Neoclassical Tearing Mode

吉田，茂樹
九州大学大学院総合理工学府

伊藤，早苗
九州大学応用力学研究所

矢木，雅敏
九州大学応用力学研究所

安積，正史
日本原子力研究開発機構

Stability Analysis of Neoclassical Tearing Mode

Shigeki YOSHIDA [*1], Sanae-I. ITOH [*2], Masatoshi YAGI[*2],

and Masafumi AZUMI[*3]

E-mail of corresponding author: *shigeki@riam.kyushu-u.ac.jp*

Abstract

Linear stability analysis of neoclassical tearing mode(NTM) is performed on the basis of four-field reduced magnetohydrodynamic(MHD) model which takes account of fluctuating ion parallel flow and ion neoclassical viscosity. The dependence of the growth rate on the kinetic effects is investigated. It is shown that the linear NTM is stabilized by ion neoclassical viscosity and that the stabilizing effect of ion parallel compressibility is weak in low collisionality regime. The coexistence of ion and electron diamagnetic drifts causes the stability.

Key words : *neoclassical tearing mode, free energy source, ion neoclassical viscosity, ion neoclassical flow, plasma β value, pressure gradient, four-field model*

1. Introduction

Various types of transition phenomena are observed in high temperature tokamak plasmas, associated with the structural formations such as the magnetic islands [1]-[6]. Due to the formation of islands, the plasma confinement is degraded or sometimes discharges become disruptive. The disruption is a combination of MHD and transition phenomena, and its relation to the linear stability of some modes is not clearly known. In TFTR (Tokamak Fusion Test Reactor in Princeton Plasma Physics Laboratory), tearing modes has been observed in the most high confinement operation regimes [7]. Significant degradation of confinement occurs by appearance of magnetic island. In JT-60 experiments, the magnetic island has been also observed and the measurement of β value normalized by poloidal magnetic field at the mode onset is performed [4] [5]. In these experiments, distinct changes of the pressure and pressure gradient are not observed, nevertheless the mode rapidly grows associated with discontinuous and large change of the growth rate. In the conventional theoretical models based on the linear instability, the temporal change of the linear growth rate should follow the change of the global plasma parameters. Namely, the abrupt change of the growth rate requires the corresponding changes of the global parameters such as safety factor q, pressure

gradient p' and so on.

Another features of the collapse phenomena are the probabilistic excitation and hysteresis nature. In high temperature plasma, the magnetic island is observed in high β operations.

In order to achieve high performance in fusion plasmas, it is necessary to understand (1) the physical mechanism of island excitation and its saturation level in high β plasma and (2) that of the associated collapse phenomena. Several theoretical works of neoclassical tearing mode (NTM) have been done [8][9][10]. In the conventional analysis, the linear stability is considered for the tearing mode. However, the experimental result also shows the linear tearing mode is stable, or, that the most unstable mode is not necessarily exited. Therefore, a certain nonlinear excitation mechanism which is beyond the linear theory's is needed to explain such a mechanism for the acceleration of the trigger mode.

It is found that saturated island width, which is determined by the competition between the bootstrap current and the free energy source due to the current density gradient is not inconsistent with experimental observations [7]. However, the onset condition or these dynamics are not fully understood from the view point of conventional analysis. In the previous analyses of NTM based on three-field model, only the electron neoclassical viscosity is included assuming that the collision frequency is larger than the rotation frequency of the NTM. Ion neoclassical viscosity is not considered in the model. This is not appropriate for the case of the high

*1 Interdisciplinary Graduate School of Engineering Sciences, Kyushu University
*2 Research Institute for Applied Mechanics, Kyushu University
*3 Japan Atomic Energy Research Institute

temperature collisionless plasma. In addition, in order to examine the dynamics of the island evolution, the former assumption of collision frequency is not valid with respect to the timescale. In this thesis, we examine the stability of NTM based on the four-field reduced MHD model. Where the ion parallel flow, ion neoclassical viscosity, and the parallel compressibility are included. In the linear analysis, these effects stabilize the NTM and the ion neoclassical viscosity strongly contributes the stabilization.

This thesis is organized as follows. In Chapter 2., we review collapse phenomena in high temperature tokamak plasma such as sawtooth oscillation and the tearing mode. Theoretical approaches based on linear or nonlinear theory of tearing modes are also explained. In Chapter 3., linear analysis of NTM based on four-field reduced MHD equation is performed. The comparison of results from three-field model with those are discussed. Dependence of growth rate on various parameters are investigated. Finally, in Chapter 4., summary and discussion are given.

2. Reviews

Various types of collapse events in toroidal plasmas have been reported in a review paper[1]. In this chapter, we review the magnetic reconnection and tearing mode instability in high temperature tokamak plasmas as examples of such collapse events. Table 1 shows the characteristics of crash events, precursors and triggering mode.

Name	Observed response	Time scale	Trigger mode	Precursor mode	Note
Sawtooth	$T_e n_e$ $\Delta q \sim 0.05$	$<100\ \mu s$	$m/n = 1/1$ etc (?)	$m/n = 1/1$	No full reconnection $q(0) <$
Partial sawtooth	As above	←	←	←	←
Disruption (thermal quench)	T_e	10-100 μs	$m/n = 1/1$ 'erosion'	$m/n = 2/1$ 3/1 etc	Density $q = 2.$
High-β collapse (tokamak)	T_e (Ti)	$<100\ \mu s$	$n \gg 1$ ballooning	$m/n = 1/1$ etc	$\beta \sim \beta_c^{id}$
Internal collapse (Heliotron)	T_e	$<100\ \mu s$	$m/n = 2/1$ interchange	$m/n = 2/1$	
ELMs (type-I)	$T_e T_i n_e$	10-100 μs	$n \gg 1$	—	$\alpha \sim \alpha_c^{id}$
X-event	$n T_i$	$<100\ \mu s$	—	—	High-T_i
BLM	∇T_e	$<100\ \mu s$	$m/n = 3/1$ Internal?	—	High-β_p
MTE	∇V_ϕ	$<100\ \mu s$	$n \gg 1$	—	Prohibic VH-max
CHS burst	$\phi(r)$	few 100 μs	$m/n = 2/2$	$m/n = 2/1$	NBI inj
IRE	t_i				Low-q_a radio tol

Table 1 Crash events, precursors and triggering modes. Abbreviations:ELMs(edge-localized modes), MTE(momentum transfer events),BLM(barrier-localized mode), IRE(internal reconnection events).(cited from Ref. [1])

2.1 Trigger Events

One of the most important issue in confinement plasmas is the abruptness of the growth of perturbations that lead to collapse. The fast sawtooth collapse is a typical example. This phenomenon is known that the $m/n = 1/1$ helical magnetic perturbation precedes the decay of the central electron temperature, where m is the poloidal mode number and n is the toroidal mode number. This perturbation is called as a precursor [11]. The observation of the precursor stimulated the study of the $m/n = 1/1$ instabilities in tokamaks [12][13]. Precise measurements of the development of the helical deformation have been made over the years. A typical example from the JET tokamak is shown in Figure 1. The helical shift of the peak of the Soft Xray-emission
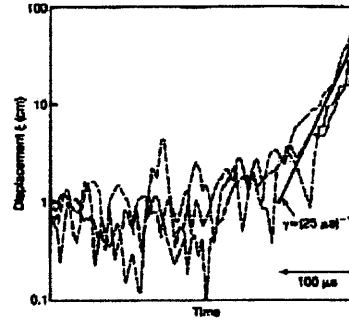

Fig. 1 Displacement of the soft x-ray emission peak during a fast sawtooth collapse observed on the JET tokamak (cited from [1]).

intensity is plotted as a function of time. In the precursor phase, the helical shift is in the range of 1-3 cm and grows very slowly. The helical deformation, at some instant, abruptly starts to grow. If one plots the temporal evolution of the growth rate of the helical deformation, it suddenly changes in an unpredictable manner, as is illustrated in Figure 2. Tearing type mode is also consider to be one of the trigger modes.

2.2 Measurement of Magnetic Islands

The magnetic island is widely observed in high β tokamak plasmas. This structure is formed by the reconnection of the poloidal magnetic field line. Figure 3 shows the three-dimensional structure of $m/n = 2/1$ magnetic island in toroidal plasma. Inside an island, it is considered that the temperature is flattened. The excitation of these islands is a result of a difference in the response of electrons and ions to the fluctuating electric field. Tearing modes have been observed and analyzed in the most high confinement operation in TFTR [7][14]. The island width determines the level of the degrada-
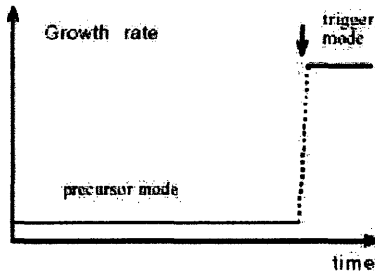
Fig. 2 Abrupt increment of the growth rate takes place at the onset of the crash. The preceding activities (precursor) have very small growth rates. The trigger mode has a large growth rate that is often of that of the order of the ideal MHD instabilities (cited from [1]).
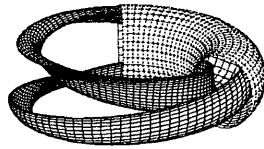

Fig. 3 The three-dimensional structure of the $m/n = 2/1$ island in a toroidal plasma.

tion of plasma confinement. Therefore, it is important that the physical mechanism is clarified.

The different kinds of methods have been used to measure the magnetic island width: external magnetic measurement, internal local temperature measurement from electron cyclotron emission (ECE) diagnostic and a direct measurement from a major radius shift experiment("Jog" experiments). Figure 4 shows a typical neutral-beam heated, high-performance discharge [15] accompanied with a $m/n = 3/2$ mode. Significant degradation in the Troyon-normalized β $[\beta_N = \beta_t a(m)B_t(T)/I_p(MA)]$ and neutron rate have been observed, which are correlated with the MHD phenomena. The Fourier spectrum evolution from one measurement coil is shown in Figure 4(b). The 3/2 mode starts at about 3.8s (300ms after NBI) preceded by an $m/n = 1/1$ fishbone-like mode [14]. There is a ~ 150 ms overlap period where both modes co-exist. The 3/2 mode decays after the NB phase and is terminated by the injection of Lithium pellet at 5.03 s.
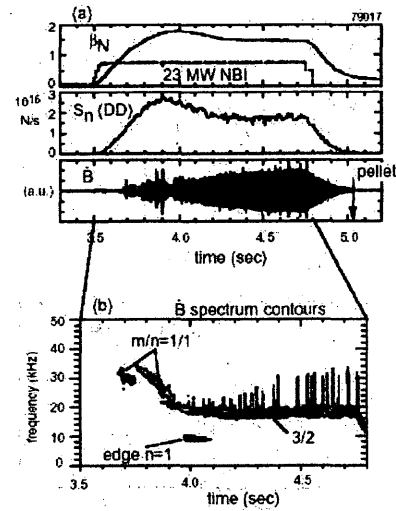

Fig. 4 Typical neutral-beam heated, high-performance discharge [15] that developed a $m/n = 3/2$ mode. Significant degradation β_N and neutron rate are showed. (cited from [7])

Magnetic island width is given by using the standard cylindrical formula as,

$$W = \sqrt{\frac{1}{m}\frac{\tilde{B}_r}{B_\theta}\frac{q}{|q'|r}} \quad \text{at } r = r_s \tag{1}$$

where $\tilde{B}_r$ is the radial component of the magnetic fluctuation. B_θ is the equilibrium poloidal field, q is the safety factor, $q' = dq/dr$, r_s denotes the radial location of rational surface. $\tilde{B}_r$ can be calculated numerically by solving the MHD equation:

$$r\frac{d}{dr}r\frac{d\tilde{\psi}}{dr} - m^2\tilde{\psi} - \frac{q}{1-nq/m}r\frac{d}{dr}\left(\frac{1}{r}\frac{d}{dr}\frac{r^2}{q}\right)\tilde{\psi} \equiv 0(2)$$

$\tilde{\psi}$ is the perturbed poloidal magnetic flux, related to the magnetic perturbation through $\tilde{B} = \nabla\tilde{\psi}\times\hat{z}$, i.e., $\tilde{B}_\theta = -\partial\tilde{\psi}/\partial r$, $\tilde{B}_r = im\tilde{\psi}/r$. The island width of an MHD mode would be referred from the "flat spot" in electron temperature profile using ECE(electron-cyclotron-emission) diagnostics. Figure 5([14]) shows comparison of thus obtained magnetic calculation with data from the ECE measurement, where (a) and (b) show the island evolution of $m/n = 3/2$ nd $m/n = 4/3$ respectively. As we can see in Figure 5 the two independent measurements are in good agreement for both $m/n = 3/2, 4/3$ cases.

2.3 FKR Theory of Tearing Mode

Magnetohydrodynamic modes in current-carrying toroidal plasma, including the ordinary infinite-conductivity kink mode and the kink-like tearing mode
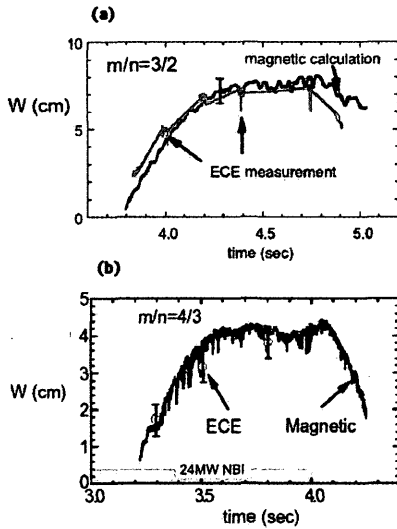
(a)

(b)

Fig. 5   Comparison of the magnetic calculation with ECE measurement. (a) and (b) are $m/n = 3/2$ and $m/n = 4/3$ islands respectively. Similar agreements have been found in these cases.(cited from [14])

have been studied. In this section, we review the linear stability analysis of the resistive tearing mode.

The original analysis of Furth, Killeen, Rosenbluth, which we shall refer to as FKR theory [16], is based on a resistive MHD model with a simple Ohm's law, $\mathbf{E} + c^{-1}\mathbf{v} \times \mathbf{B} = \eta\mathbf{J}$, where $\mathbf{B}$ and $\mathbf{E}$ are the electric and magnetic field, $\mathbf{v}$ is the fluid velocity, $\mathbf{J}$ is the electrical current density and η is the electrical resistivity. The hydromagnetic approximation is assumed to be valid, and the ion pressure and inertia terms are neglected in Ohm's law.

$$\partial\mathbf{B}/\partial t = \nabla \times (\mathbf{v} \times \mathbf{B}) - \nabla \times [(\eta/4\pi)\nabla \times \mathbf{B}]. \quad (3)$$

An isotropic resistivity and the mass of the electrons in Eq.3 is neglected. If the electron-inertia term is included in the equation, it gives rise to a tearing mode in collisionless limit. Additionally, viscosity is neglected, so that the equation of motion may be written as

$$\nabla \times (\rho d\mathbf{v}/dt) = \nabla \times [(1/4\pi)(\nabla \times \mathbf{B}) \times \mathbf{B} + \mathbf{g}\rho] \quad (4)$$

where ρ is the mass density and $\mathbf{g}$ the acceleration due to gravity. As usual, the $\mathbf{g}\rho$ term may be interpreted as resulting from acceleration of the current layer, or from the interaction of a plasma pressure gradient and a slight curvature of the current layer. The FKR theory basically consists of these equations and continuity equation

$$\partial(\mathbf{g}\rho)/\partial t + \mathbf{v} \cdot \nabla(\mathbf{g}\rho) = 0 \quad (5)$$

on the assumption that the fluids is incompressible, namely, $\nabla \cdot \mathbf{v} = 0$. From the FKR theory, if the resistivity is the main cause of the dissipation (for large $S = \tau_R/\tau_H$) and the growth rate of the island is estimated by

$$\gamma \sim \tau_R^{-3/5}\tau_H^{-2/5} \quad (6)$$

$$(\tau_R = 4\pi a^2/\eta, \quad (7)$$
$$> \tau_H = a(4\pi\rho)^{1/2}/B)$$

where τ_R, τ_H and a are resistive diffusion time, hydromagnetic transit time, and a measure of the thickness of the current layer. However, this estimation does not completely explain the observations which are reviewed in section 2.1 and 2.2. Nonlinear analysis is needed for understanding the acceleration of trigger mode as well as the saturation mechanism of magnetic island. Also, the neoclassical effect on tearing mode (driven not only by current diffusivity but also by pressure gradient) should be taken into account.

2.4   Boundary Layer Problem

The parameter $S = \tau_R/\tau_H = aB/\eta(4\pi/\rho)^{1/2}$ is the magnetic Reynolds number. To illustrate the boundary layer nature of the problem for $\eta \to 0$ and $S = \tau_R/\tau_H \to \infty$, we consider the induction equation in the Cartesian coordinates in a slab geometry,

$$\partial B_{x1}/\partial t = i(\mathbf{k} \cdot \mathbf{B_0})v_{x1} + \eta_0/4\pi\nabla^2 B_{x1} \quad (8)$$

where η_0 is assumed uniform for simplicity . Since $S \gg 1$, flux-freezing characterized by $\partial B_{x1}/\partial t \sim i(\mathbf{k} \cdot \mathbf{B_0})v_{x1}$ will hold to a good approximation everywhere except in the neighborhood of the resonant surface where $F \equiv \mathbf{k} \cdot \mathbf{B_0}/(kB) = 0$. Near this surface, the first term of right hand side in Equation 8 is small and all three terms will be comparable in magnitude. Since η_0 is small, this implies that $\nabla^2 B_{x1}$, and hence $d^2 B_{x1}(x)/dx^2$, must become locally very large in a narrow resistive layer where $F = 0$ holds. States away from $F = 0$ may be described by the infinite conductivity limit. On the other hand, resistivity effects is taken into consideration only in a narrow boundary layer about $F = 0$. Considering on the scale of the current layer, the perturbed field component $\psi \equiv B_{x1}(x)/B$ appears to have a discontinuity in its first derivative given by

$$\Delta' = \frac{\psi'(0+) - \psi'(0-)}{\psi(0)} = \left[\frac{d}{dx}\log\psi\right]_{0-}^{0+} \quad (9)$$

across the surface $F = 0$, which we take without loss of generality to be $x = 0$.

Note that Δ' indicates the free energy source. The growth rates of the resistive modes are then determined

by requiring that the discontinuity of the "inner" solution should match that of the "outer" solution. Then we need to calculate the change in logarithmic derivative $\Delta'_{int}(\gamma)$ of the "inner" solution across the resistive layer and the growth rate γ can be obtained from the eigenvalue equation

$$\Delta'_{int}(\gamma) = \Delta'_{ext}. \tag{10}$$

2.5 Rutherford Theory of Magnetic Island

Linear analysis is applicable within a linear tearing layer around the rational surface, whose width is determined by the plasma inertia and resistivity [17]. When the magnetic island width exceeds the linear tearing layer width, the island dynamic becomes strongly nonlinear and the linear treatment breaks down. For typical plasma parameters in present-day tokamaks, the tearing layer is so thin that any visible magnetic islands have to be in the nonlinear stage.

Nonlinearity is important principally in the singular layer around $\mathbf{k} \cdot \mathbf{B} = 0$. In the case where the resistive skin diffusion time is much longer than the hydrodynamic time, the exponential growth of the field perturbation is replaced by algebraic growth like t^2 at an amplitude of order $(\tau_H/\tau_R)^{4/5}$ [17]. The relative amplitudes of the $m = 4, 3$, and 2 modes shown in Figure 6 are in good agreement with the observations [17]. The absolute amplitudes of the modes are a little larger than those of the observations. Figure 6 also shows that there is a
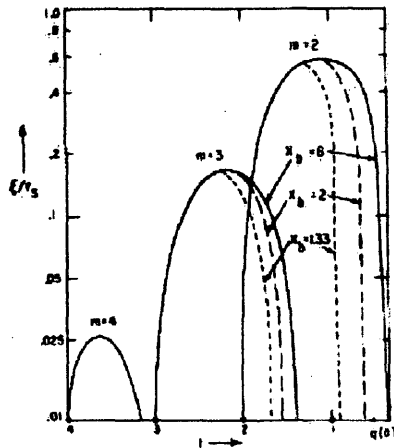
Fig. 6 Mode amplitude as functions of time for a constant current tokamak with shrinking current channel, and three locations x_b of the conducting shell. Amplitude are expressed by the half-width ξ of the magnetic island in terms of their radii r_s. Good agreements with the observed amplitudes of the $m \geq 2$ oscillations are shown.(cited from [17])

small interval of time during which both the $m = 3$ and $m = 2$ modes are present. This contradicts to the fact that the $m = 3$ mode becomes stable before the onset of the $m = 2$, if the linear stability criteria is taken.

2.6 Renormalized Theory

Nonlinear analysis of anomalous tearing mode known as renoramlized theory have been developed in recent years [18]. The theory predicts two principal nonlinear effects: an anomalous flux diffusivity due to turbulent fluid convection in Ohm's law and a vorticity damping term due to turbulent magnetic stresses in the equation of motion. Many numerical calculations of multi helicity tearing interaction have been done [19]. Effects such as resistivity evolution [20], toroidicity [21], noncircularity of the plasma cross section [22], and diamagnetic rotation [23] have been included. It has been shown that they do not modify the basic dynamical mechanism of the nonlinear interaction of tearing modes. Therefore, in the recent study, the large aspect ratio, reduced set of resistive MHD equations applied to cylindrical geometry is considered [18].

The sequence of phenomena leading to the final disruptive phases is shown in Figure 7(cited from [18]). First, following the overlap of the 2/1 and 3/2 mag-
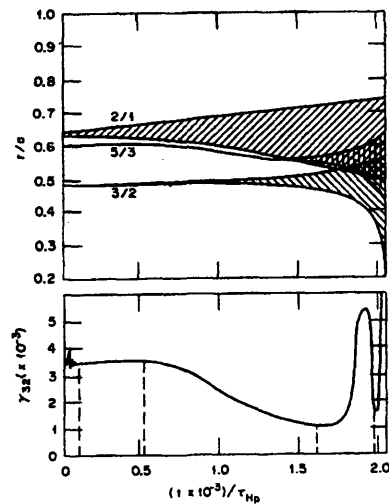
Fig. 7 The calculations are performed in such a way that the various physical effects appear as a sequence of events. (a)The radial extent of three magnetic islands. (b)The instantaneous growth rate of the 3/2 mode. The overlap of magnetic islands of 2/1 and 5/3 generates the magnetic stochasticity and accelerates the growth of 3/2 mode. (cited from [18])

netic island, the large current gradient that develops in the region between the two islands results in a

positive Δ' for the nonlinearly driven 5/3 fluctuation. The nonlinear drive is a consequence of the overlap of the 2/1 and 3/2 modes. The resonant mode coupling of the 2/1 mode with the 5/3 mode then results in the rapid, nonlinear destabilization of the 3/2 mode. These nonlinear interactions are treated by one-point renormalization method [18]. The direct interactions of the test mode with background fluctuations are reduced to the form of anomalous diffusivities, and the anomalous tearing mode growth rate is given as $\gamma \sim \left(\sum_{k'} k_\theta'^2 |\phi_{k'}|^2 \right)^{\frac{3}{8}} (\Delta')^{\frac{1}{2}}$ which means that the background fluctuations contribute to the anomalous resistivity and accelerate the mode growth through the nonlinearity. The anomalous growth rate of the 3/2 mode is calculated and its value is compared with the nonlinear growth rate of this mode (Figure 8). The good
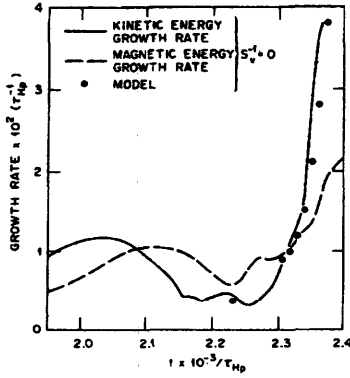

Fig. 8   The growth rate of the 3/2 mode as obtained from the model is compared with the calculation. (cited from [18])

agreement is shown and it is also important to investigate the correlation of this anomalous growth with the buildup of the high-m fluid turbulence. This is one of theoretical models which explains the mode acceleration mechanism, however, the rapid growth of trigger mode with a single helicity has not explicitly shown.

3.   Linear Analysis of NTM based on the Four-field Reduced Neoclassical MHD equation

3.1   Four-field MHD equation

We consider a high temperature plasma of major and minor radii R_0 and a with a toroidal magnetic field B_0 in the cylindrical coordinates (r, θ, z). To analyze the linear NTM, the four-field reduced neoclassical MHD model is introduced[24] . This model consists of the vorticity equation:

$$\frac{\partial}{\partial t}\nabla_\perp^2 F + [F, \nabla_\perp^2 F] - \alpha_i \nabla_\perp \cdot [p, \nabla_\perp F]$$

$$= -\nabla_\parallel \nabla_\perp^2 A - [\Omega, p] + \mu_i^{cl} \nabla_\perp^4 F$$
$$- \frac{q}{\epsilon}\mu_i^{neo}\frac{\partial U_{pi}}{\partial r} - \frac{q}{\epsilon}\frac{m_e}{m_i}\mu_e^{neo}\frac{\partial U_{pe}}{\partial r}, \tag{11}$$

Ohm's law:

$$\frac{\partial}{\partial t}(A - \alpha^2 \frac{m_e}{m_i}\nabla_\perp^2 A)$$
$$= -\nabla_\parallel(\phi - \alpha_e p) + \alpha^2 \frac{m_e}{m_i}[\phi, \nabla_\perp^2 A] + \eta_\parallel^{cl}\nabla_\perp^2 A$$
$$- 4\mu_e^{cl}\alpha^2 \frac{m_e}{m_i}\nabla_\perp^4 A + \alpha h_{BS}\frac{m_e}{m_i}\mu_e^{neo}U_{pe}, \tag{12}$$

the evolution of ion parallel velocity:

$$\frac{\partial}{\partial t}v_\parallel + [\phi, v_\parallel] = -\nabla_\parallel p + 4\mu_i^{cl}\nabla_\perp^2 v_\parallel$$
$$- \mu_i^{neo}U_{pi} - \frac{m_e}{m_i}\mu_e^{neo}U_{pe}, \tag{13}$$

and the electron continuity equation:

$$\frac{\partial}{\partial t}p + [\phi, p] = \hat{\beta}([\Omega, \phi - \alpha_e p] - \nabla_\parallel(v_\parallel + \alpha\nabla_\perp^2 A)$$
$$+ \eta_\perp^{cl}\nabla_\perp^2 p - \alpha\frac{m_e}{m_i}\frac{q}{\epsilon}\mu_e^{neo}\frac{\partial U_{pe}}{\partial r}), \tag{14}$$

where

$$F = \phi + \alpha_i p, \tag{15}$$

$$U_{pi} = v_\parallel + \frac{q}{\epsilon}\frac{\partial}{\partial r}(\phi + \alpha_i p), \tag{16}$$

$$U_{pe} = v_\parallel + \alpha\nabla_\perp^2 A + \frac{q}{\epsilon}\frac{\partial}{\partial r}(\phi - \alpha_e p); \tag{17}$$

$$\Omega = 2r\cos\theta, \quad \hat{\beta} = \frac{\beta}{1 + \beta}, \quad \alpha = \frac{c}{a\omega_{pi}},$$

$$\alpha_i = \frac{T_i}{T_i + T_e}\alpha, \alpha_e = \frac{T_e}{T_i + T_e}\alpha,$$

and

$$\nabla_\parallel = \frac{\partial}{\partial z} - [A,]. \tag{18}$$

The closed set of equations Equation11-14 is called as 'four-field model' in the following calculations. On the other hand, the approximations $\nabla_\parallel v = 0$ and $U_{pi} = 0$ give the three-field closed set of equations, in which only the electron neoclassical viscosity is kept. We call these equations as 'three-field model'. The variables of four-field $\{\phi, A, v_\parallel, p\}$ are the fluctuating electrostatic potential, vector potential parallel to the magnetic field, parallel velocity and electron density, respectively. In this model, the ion and electron temperatures T_i and T_e are assumed to be constant and uniform. The coefficients $\{\mu_i^{cl}, \mu_e^{cl}, \eta_\parallel^{cl}, D_{cl}\}$ are classical ion viscosity, electron viscosity(hyper-resistivity), resistivity and diffusivity[25]. α is the normalized ion skin depth $(c/a\omega_{pi})$, and Ω is the normalized magnetic curvature, which introduces the ballooning coupling. $\{q, \epsilon, \omega_{pi}, \beta\}$ indicates safety factor, inverse aspect ratio, ion plasma frequency and plasma beta value respectively. The Poisson bracket is defined by $[f, g] = \mathbf{b} \cdot \nabla f \times \nabla g$ where $\mathbf{b}$ is an unit vector parallel to the magnetic field. These

equations are normalized by toroidal Alfven time and minor radius. The explicit forms are given as follows;

$$\frac{\epsilon v_A}{a}t \rightarrow t, \qquad \frac{r}{a} \rightarrow r,$$

$$\frac{\phi}{B_0 \epsilon a v_A} \rightarrow \phi, \qquad \frac{A}{\epsilon a B_0} \rightarrow A, \qquad \frac{\mu_0}{B_0^2 \epsilon}p \rightarrow p, \quad (19)$$

$$\frac{\eta_c}{\mu_0 \epsilon a v_A} \rightarrow \eta_{c,}, \qquad \frac{\mu_c}{n_0 m_i \epsilon a v_A} \rightarrow \mu_c, \qquad \frac{\chi_c}{\epsilon a v_A} \rightarrow \chi_c,$$

where v_A is Alfven velocity ($v_A = B/\sqrt{\mu_0 \rho}$). The electron inertia terms are included in Equation 12, which are negligibly small in the linear regime. The energy conservation relation is written by

$$H = \frac{1}{2} \int d^3 x (|\nabla_\perp F|^2 + |\nabla_\perp A|^2 + |v_\parallel|^2$$

$$+ \frac{|p|^2}{\beta} + \alpha^2 \frac{m_i}{m_e}|\nabla_\perp^2 A|^2), \qquad (20)$$

$$\frac{dH}{dt} = - \int d^3 x (\mu_i^{cl}|\nabla_\perp^2 F|^2 + \eta_\parallel^{cl}|\nabla_\perp^2 A|^2$$

$$+ 4\mu_i^{cl}|\nabla_\perp v_\parallel|^2 + \eta_\perp^{cl}|\nabla_\perp p|^2 + 4\mu_e \alpha^2 \frac{m_e}{m_i}|\nabla_\perp \nabla_\perp^2 A|^2$$

$$+ \mu_i^{neo}|U_{pi}|^2 + \frac{m_e}{m_i}\mu_e^{neo}|U_{pe}|^2). \qquad (21)$$

In this analysis, the flux surface averaged part of the neoclassical viscous tensor is incorporated[24, 26]. The parallel and cross viscous stress terms are approximated as,

$$\mathbf{b} \cdot \nabla \cdot \Pi_{\parallel s} \simeq m_s n_s \mu_s B^2 U_{ps}, \qquad (22)$$

$$\nabla \cdot (\mathbf{b} \times \nabla \cdot \Pi_{\parallel s}) \simeq -\frac{B_0}{B_\theta}\frac{\partial}{\partial r}(\mathbf{b} \cdot \nabla \cdot \Pi_{\parallel s}), \qquad (23)$$

where the suffix s denotes species of charged particle. The neoclassical viscosities are given by the interpolated formula according to [27] as

$$\mu_e^{neo} = \frac{2.3\sqrt{\epsilon}\nu_e}{(1 + 1.07\nu_{e*}^{1/2} + 1.02\nu_{e*})(1 + 1.07\nu_{e*}\epsilon^{3/2})}, \qquad (24)$$

$$\mu_i^{neo} = \frac{0.66\sqrt{\epsilon}\nu_i}{(1 + 1.03\nu_{i*}^{1/2} + 0.31\nu_{i*})(1 + 0.66\nu_{i*}\epsilon^{3/2})}, \qquad (25)$$

where $\nu_{s*} = \nu_s/(\epsilon^{3/2})(qR)/v_{ths}$, v_{ths} is thermal velocity described by $v_{ths} = \sqrt{2T_s/m_s}$. These viscosities are assumed to be constant, since the viscous terms have influence on the NTM only at the rational surface and profile effects are less important for the NTM.

3.2 Numerical Analysis

A perturbed quantity $f(x, t)$ is assumed to vary as $f_{m,n}(r)exp[im\theta + inz + (\gamma - i\omega)t]$ in the cylindrical coordinates, where m is a poloidal mode number, n is a toroidal mode number, γ is the growth rate and ω is the rotation frequency of the linear tearing mode. The direction of $\omega > 0$ is electron diamagnetic drift direction and that of $\omega < 0$ is ion diamagnetic drift direction. $f_{m,n}(r)$ satisfies the boundary conditions; $f_{m,n}(0) = 0$

and $f_{m,n}(a) = 0$. In this study a single helicity mode with $(m, n) = (2, 1)$ is considered. The basic equations Equation11-14 are linearized and the linear contribution from the ion convective term $[F, \nabla_\perp^2 F]$ and gyro-viscous term $\alpha_i \nabla_\perp \cdot [p, \nabla F]$ are reduced as,

$$[F, \nabla_\perp^2 F] - \alpha_i \nabla_\perp \cdot [p, \nabla F]$$

$$= \frac{\alpha_i}{r}\left\{-\frac{d^3 p_0}{dr^3}\frac{\partial\phi}{\partial\theta} + \frac{dp_0}{dr}\frac{1}{r}\frac{\partial^2\phi}{\partial\theta\partial r} - \frac{d^2 p_0}{dr^2}\frac{\partial^2\phi}{\partial\theta\partial r}\right\}. \qquad (26)$$

The electron collision frequency ν_e is the basic parameter which determines the strength of the neoclassical viscosity. The coefficients of the neoclassical viscosities and total resistivity as a function of the electron collision frequency are calculated from equations Equation11-14 shown in Figure 9. Four-field reduced
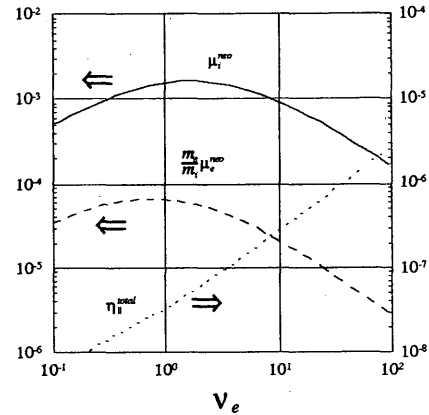

Fig. 9   The collisionality dependencies of the neoclassical viscosities and total resistivity ($\eta_\parallel^{total} \equiv \eta_\parallel^{cl} + \eta_\parallel^{neo}$). The electron collision frequency ν_e is normalized by the toroidal Alfven time. $\nu_e \sim 1$ corresponds to the plateau regime. The high temperature plasma lies in the banana regime($\nu_e < 1$)

MHD model $\{\phi, A, v_\parallel, p\}$ is numerically solved via matrix method with inverse iteration and these eigen values are evaluated. The safety factor profile is given as

$$q(r) = \frac{q(r_s) - q(0)}{2^b - 1}\left(1 + \left(\frac{r}{r_s}\right)^a\right)^b$$

$$+ q(0) - \frac{q(r_s) - q(0)}{2^b - 1} \qquad (27)$$

where r_s is rational surface. The magnetic shear parameter s is changed in accordance with the variations of a and b or $q(0)$. We set $a = 3.0, b = 1.0, q(0) = 1.2$ as default values. Figure 10 shows safety factor profiles in cases with $q(0) = 1.2, 1.4$ and 1.6.

The case with $q(0) = 1.2, q(r_s) = 2.0$, corresponds to $s(r_s) = 1.2$ Other plasma parameters are given by
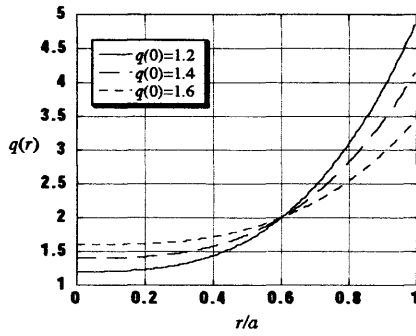
Fig. 10 The safety profiles $q(r)$ are shown for the case of $q(0) = 1.2, 1.4$ and 1.6. The corresponding values of local shear $s(r_s)$ at the rational surface are $s = 1.2, 0.9$ and 0.6 respectively.

$\beta = 0.01, \alpha = 0.01, \epsilon = 1/3$ and $T_e = T_i = const..$ Figure 11 shows typical radial eigenmode functions of linear NTM for the case with $\nu_e = 0.7$.
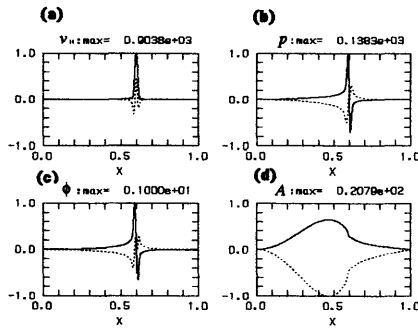

Fig. 11 Typical eigenmode profiles of linear NTM in the four-field model. The electron collision frequency is chosen to $\nu_e = 0.7$ as the normalized value. The eigenmode profile is normalized by the maximum amplitude of each value. The relative amplitudes of the fluctuations are $F_{max} = 1, A_{max} = 20.8, p_{max} = 13.8 \times 10^2$ and $v_{max} = 90.4 \times 10^2$. $v_{\parallel}$ which is not considered in three-field model has big amplitude at rational surface ($r_s = 0.6$).

Figure 11 (a), (b), (c), (d) indicate the eigen functions of $v_{\parallel}, p, F, A$ respectively. Solid line and dashed line indicate the real and imaginary part of eigen function respectively. The eigenmode profile is normalized by the maximum amplitude of each value. Fluctuating ion parallel velocity $v_{\parallel}$ which couples with density perturbation through the parallel compressibility has a large amplitude at the rational surface. It is seen that F and p are localized at the rational surface ($r_s = 0.6$)

from Figure 11, (a) (b) and the radial derivative of the vector potential $dA(r)/dr$ is discontinues at the rational surface (Figure 11 (c)). These features show the typical mode structures of tearing mode.

3.2.1 Dependence of Growth Rate on Free Energy Source

The magnetic shear s indicates the gradient of safety factor profile at the rational surface, which is given by

$$s = \frac{r_s}{q(r_s)} \frac{dq(r_s)}{dr_s}. \tag{28}$$

In our model, s changes according to the change of $q(0)$. The shear parameter decreases as safety factor profile is flattened. The values of local shear parameter $s(r_s)$ are given by $1.2, 0.9$ and 0.6, for $q(0) = 1.2, 1.4, 1.6$, respectively. The parameter Δ' is known parameter to indicate the free energy source of tearing mode. It is defined by the jump of derivative of vector potential A at the rational surface r_s as

$$\Delta' \equiv \frac{A'(r_s + 0) - A'(r_s - 0)}{A(r_s)}. \tag{29}$$

The vector potential in the ideal region (outer region of singular layer) can be calculated from the following equation,

$$\frac{d^2}{dr^2} A = -\frac{1}{r} \frac{d}{dr} A + \left(\frac{3}{r} \frac{k'_{\parallel}}{k_{\parallel}} + \frac{k''_{\parallel}}{k_{\parallel}} + \frac{m^2}{r^2} \right) A \tag{30}$$

Δ' is determined by connecting these inner and outer solutions in the limit of $r \to r_s$. Generally speaking, if Δ' is positive, the NTM is unstable while if Δ' is negative, the NTM is stable. Figure 12 shows the dependence of Δ' on the shear parameter. It is seen that
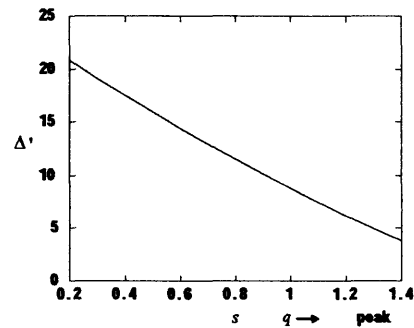

Fig. 12 The dependencies on free energy source Δ' of the growth rate γ for the cases with three-field and four-field are compared, where we set $\beta = 0.01, \alpha = 0.01, \alpha_i = \alpha_e = \alpha/2$.

Δ' decreases monotonously as the shear parameter increases. In other words, Δ' decreases monotonously as

the profile of safety factor is peaked. Figure 13 shows the dependencies of the growth rate (a) and the rotation frequency (b) on the collisionality for various $q(0)$ values. It is found that tearing mode tend to be unstable
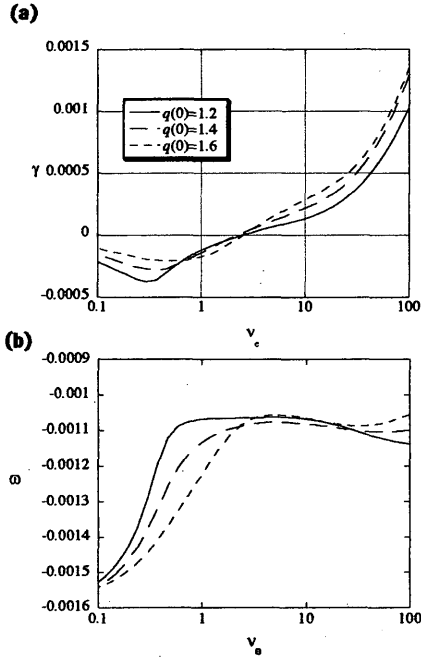
(a)

(b)

Fig. 13   The dependencies on collisionality of the growth rate γ (a) and the rotation frequency ω (b) for the cases of various $q(0)$ value. The local shear parameter $s(r_s)$ are given by $1.2, 0.9, 0.6$ when $q(0) = 1.2, 1.4, 1.6$ respectively. NTM is destabilized by flattening of q-profile.

in the wide collisionality regime as q-profile is flattened. However, in $0.8 < \nu_e < 2.5$ regime (plateau regime), this tendency is changed. The threshold value of stability on ν_e doesn't change by change of q-profile. Therefore, it is not crucial to stability of the NTM.

The dependence of the growth rate on the free energy source due to the plasma current gradient Δ' is analyzed and the result is compared with those of the three-field model. Figure 14 shows the dependence of the growth rate on Δ' in the case with $\nu_e = 2.4$ (plateau regime). The dashed line and solid line indicate the results from three-field model and four-field model, respectively. In the four-field case, the threshold of the instability $\Delta'_c(\approx 10.2 > 0)$ appears while $\gamma > 0$ holds for $\Delta' > 0$ in the three-field case. In the four-field case, the threshold increases from $\Delta'_c = 0$ to $\Delta'_c = 10.2$. It is demonstrated that the ion neoclassical viscosity and parallel compressibility, which are newly introduced in the four-field model, have stabilizing effects on the NTM.
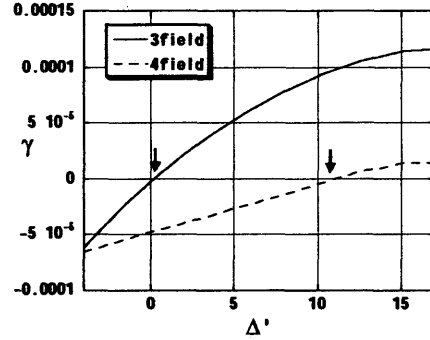

Fig. 14   The dependencies on free energy source Δ' of the growth rate γ for the cases with three-field and four-field are compared, where we set $\beta = 0.01, \alpha = 0.01, \alpha_i = \alpha_e = \alpha/2$.

3.2.2   Stabilization Mechanism of NTM in Four-field Model

In order to clarify the stabilization effects on the NTM in the four-field model, the dependence of the growth rate on the ion neoclassical viscosity is separately investigated. Figure 15 shows the dependence of the growth rate on the collisionality. The solid line, dashed line and long dashed line indicate the results in the cases with four-field model, three-field model and four-field model without ion neoclassical viscosity, respectively. In the three-field model case, the NTM is unstable in the entire collisionality regime. In the four-field model, the NTM is stabilized by ion neoclassical viscosity and parallel compressibility in the low collisionality regime (i.e. banana-plateau regime). In the four-field model without ion neoclassical viscosity case, the effect of parallel compressibility exists. However, comparing the four-field model without ion neoclassical case with the three-field model, it is found that the compressibility effect is weak. Namely, from the comparison study between three-field model and four-field model without ion neoclassical viscosity cases, it is concluded that the stabilization effect of compressibility is not crucial to the stability of NTM. In other words, NTM is more strongly stabilized by the ion neoclassical viscosity than by the parallel compressibility.

3.2.3   Dependence of Growth Rate on Various Parameters

The dependence of the growth rate on various parameters are investigated based on four-field model. At first, the effect of fluctuating bootstrap current on the NTM is analyzed. The last term of right hand side in Ohm's law, Equation 12, represents the fluctuating bootstrap current term. Changing the coefficient
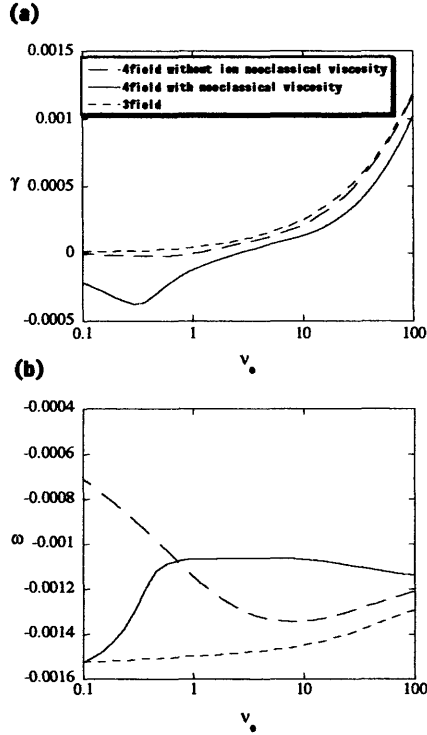
(a)

(b)

Fig. 15   The dependencies on collisionality of γ (a) and ω (b) for the cases with three and four-field. The solid line, dashed line and long dashed line indicate the results for the case of four-field model, three-field model and four-field model without ion neoclassical viscosity, respectively. Where, ion finite Larmor radius effect and electron diamagnetic drift effect are included in each case.
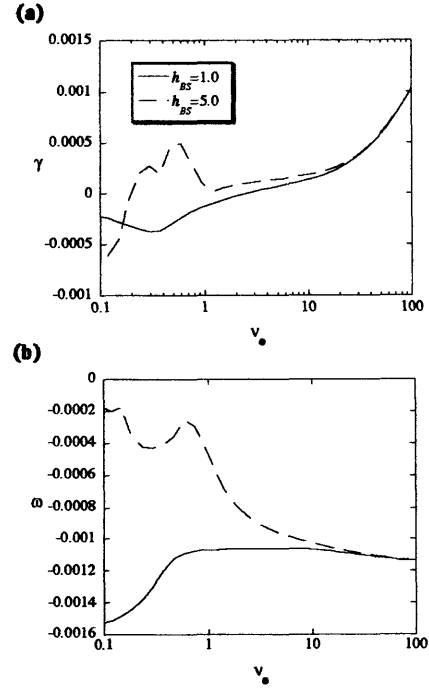
(a)

(b)

Fig. 16   The dependencies on collisionality of γ (a) and ω (b). The solid line and dashed line indicate the results for the case with $h_{BS} = 1.0, h_{BS} = 5.0$, respectively.

h_{BS}, where h_{BS} is the parameter which determines the strength of fluctuation bootstrap current, (*i.e.*, the effective pressure gradient at the rational surface), we exame this effect. Figure 16 shows the dependence of the growth rate on the collisionality for $h_{BS} = 1.0$ and $h_{BS} = 5.0$. The solid line and dashed line indicate the results in cases with $h_{BS} = 1.0$, $h_{BS} = 5.0$ respectively. It is shown that the fluctuating bootstrap current destabilizes NTM in low collisionality regime while the destabilization effect is weak in high collisionality regime(classical tearing mode).

Next, the effect of the diamagnetic drift on NTM is analyzed. Essentially, two terms contribute the stability. One is the ion diamagnetic drift effect proportional to α_i which appears in the vorticity equation Equation11 and the other is the electron diamagnetic drift effect proportional to α_e in the Ohm's law Equation12. The dependence of the growth rate with/without α_i and α_e is examined for entire collisional regime. In the large

or middle size tokamak plasma, the normalized skin depth α is estimated to be $0.01 \sim 0.1$ and $\alpha_{i,e}$ to be $0.005 \sim 0.1$ for $T_i = T_e$. By use of typical values above the results are shown in Figure 17. The solid line, long dashed line and dashed line indicate the results in the cases with $\alpha_i = 0.005, \alpha_e = 0.005; \alpha_i = 0, \alpha_e = 0.005$ and $\alpha_i = 0.005, \alpha_e = 0$ respectively. Here we fix $\alpha = 0.01$ for all cases and change α_i or α_e, separately. Namely, we rewrite $\nabla_{\parallel}(\phi - \alpha_e p)$ term in Ohm's law as $\nabla_{\parallel}(F - (\alpha_e + \alpha_i)p)$. It is found that ion and electron diamagnetic drift effects stabilize the NTM. It is found that the NTM is stabilized in the low collisionality regime by the combined effect of ion neoclassical viscosity and both ion and electron diamagnetic drift. These are seen from Figures 15 and 17.

Finally, the finite-beta effect on the NTM stability is analyzed. For various value of β, the growth rates are examined. Figure 18 shows the dependence of the growth rate on the collisionality. The cases with $\beta = 0.005, 0.01$ and 0.02 are plotted. It is seen that γ decreases as β value increases and the rotation to the direction of the ion diamagnetic drift direction enhances. This result shows the finite-β stabilization effect on the NTM. It is expected that the linear NTM becomes stable as β increases and the diamagnetic drift effect be-
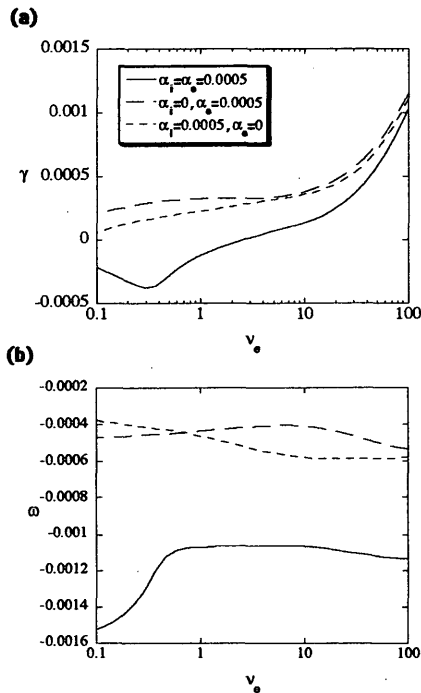
Fig. 17   The dependencies on collisionality of γ (a) and ω (b). The solid line, long dashed line and dashed line indicate the results for the case of $\alpha_i = \alpha_e = 0.005, \alpha_i = 0, \alpha_e = 0.005$ and $\alpha_i = 0.005, \alpha_e = 0$, respectively. Where, ion neoclassical viscosity effect is included in each case.

Fig. 18   The dependencies on collisionality of γ (a) and ω.The solid line, long dashed line and dashed line indicate the results for the case of $\beta = 0.005, 0.01, 0.02$, respectively.

comes strong. Figures 17(b) and 18 (b) also reveal that the NTM is stabilized as the magnetic island rotates in the direction of the ion diamagnetic drift direction.

On the other hand, the NTM is frequently observed in high β plasmas. From these observations, it is reported that NTM tends to be driven and that the island width is outspread as β increases. These results contradict to our linear four-field analysis. Therefore, the nonlinear analysis is also necessary to resolve this contradiction.

4. Summary and Discussion

The linear stability of NTM is investigated based on four-field reduced MHD equations in which ion neoclassical viscosity and fluctuating ion parallel flow are taken into account. The results are compared with those from conventional three-field model which only includes the electron neoclassical viscosity.

It is found that 1) the stable regime of NTM exists even if $\Delta' > 0$ in four field model, which shows that the careful examinations are necessary for experimental interpretations. 2) The upshifted threshold value, Δ'_c, depends on the collisionality and we obtain $\Delta'_c \approx 10.2$
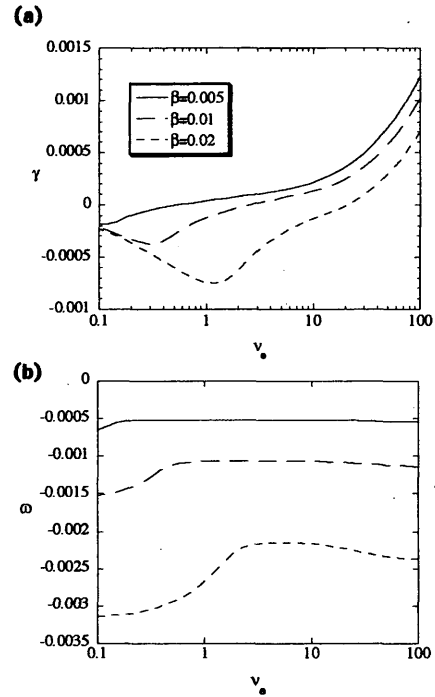
for $\nu_e = 2.4$(plateau regime).

In order to clarify whether the ion neoclassical viscosity or the ion parallel flow plays the more important role on the stabilization of NTM, the dependence on the compressibility of the growth rate without ion neoclassical viscosity is investigated. It was found that 3) the stabilization effect of ion neoclassical viscosity is much more dominant than that of the parallel compressibility in the low collisionality regime. In fact, it is considered that free energy is strongly scattered and lost by magnetic pumping(trapped ion plays important role for NTM stabilization). This stability effect is weak in the collisional regime.

Dependence of the NTM stability on various parameters are investigated based on four-field model. The fluctuating bootstrap current effect on the stability of NTM is examined. It is found that 4) the fluctuating bootstrap current destabilizes the NTM in low collisionality regime while the effect is weak in the collisional regime (classical tearing mode). This result indicates that the NTM is destabilized as the pressure gradient becomes steep. The diamagnetic drift effect was also analyzed. It is found that 5) the ion and electron diamagnetic drifts stabilize the NTM. 6) The NTM becomes stable only if the ion and electron diamagnetic drift ef-

fects and ion neoclassical drift effect coexist. Finally, the finite-beta effect is examined. 7) The NTM is stabilized by the finite-beta effect in a wide collision regime. However, in some experiments, it is observed that NTM tend to be driven as β increases. The nonlinear analysis is also necessary to resolve this contradiction.

References

1) S.-I. Itoh, K Itoh, H Zushi and A. Fukuyama, Plasma Phys. Control. Fusion Vol.40, (1998) 879.

2) S. Von Goeler, W. Stodied and N. Sauthoff, Phys. Rev. Lett. Vol.40, (1974) 1201.

3) L. A. Artsimovich, Nucl. Fusion Vol.12, (1972) 215.

4) A. Isayama, Y. Kamada, T. Ozeki and N. Isei, Nucl. Fusion Vol.41, (2001) 761.

5) JT-60 Team: Presented by S. Takeji "the Workshops on Control of Neoclassical Tearing Mode by ECH", Feb., 2001, RIAM

6) JET Team (presented by D. J. Campbell), Plasma Phys. Control. Fusion Vol.3, (1991) 231.

7) Z. Chang, J. D. Callen, E. D. Fredrickson, et al., Phys. Rev. Lett. Vol.74, (1995) 4663.

8) A. I. Smolyakov, Phys. Fluids Vol.16, (1993) 657.

9) O. Sauter et al., Phys. Plasmas Vol.4, (1997) 1654.

10) C. C. Hegna and J.D. Callen, Phys. Plasmas Vol.4, (1997) 2940.

11) K. M. McGuire and D. C. Robinson Nucl. Fusion Vol.19, (1979) 505.

12) J. A. Wesson Vol.18, (1978) 87.
    J. A. Wesson 1987 Tokmaks (Oxford: Clarendon)
    J. A. Wesson 1996 Tokamaks 2nd edn(Oxford: Clarendon)

13) R. B. White 1989 Theory of Tokamak Plasmas(Amsterdam: North-Holland).

14) Z. Chang, E. D. Fredrickson, S. H. Batha, et al., Phys. Plasmas Vol.5, (1998) 1076.

15) J. D. Strachan, M. Bitter, A. T. Ramsey, et al., Phys. Rev. Lett. Vol.58, (1987) 1004.

16) M. N. Rosenbluth, H. P. Furth and John Killeen, Physics. Fluids Vol.6, (1963) 4.

17) P. H. Rutherford Vol.16, (1973) 1903.

18) P. H. Diamond, R. D. Hazeltine, and Z. G. An Vol.27, (1984) 1449.

19) B. V. Waddell, B. A. Carreras, H. R. Hicks, and J. A. Holmes, Phys. Fluids Vol.22, (1979) 896

20) B. A. Carreras, H. R. Hicks, J. A. Holmes, and B. V. Waddell, Phys. Fluids Vol.23, (1980) 1811

21) B. A. Carreras, H. R. Hicks, and D. K. Lee, Phys. Fluids Vol.24, (1981) 66

22) B. A. Carreras, J. A. Holmes, and V. E. Lynch Vol.21, (1981) 511

23) H. R. Hicks, B. A. Carreras and J. A. Holmes, Phys. Fluids Vol.27, (1984) 909

24) J. D. Callen and K. C. Shaing, Phys. Fluids, Vol.28, (1985) 1845.

25) S. I. Braginskii: *Reviews of Plasma Physics* , edited by M. A. Leontovich, Consultant Bureau, New York(1965) Vol.1.

26) J. D. Callen, W. X. Qu et al: *Proc. of the 11th International Conference on Plasma Physics and Controlled Nuclear Fusion Research*, Vol.2, (1987) 149

27) F. L. Hinton and R. D. Hazeltine, Rev. Mod. Phys. Vol.48, (1976) 239